Supporting Information

Sandwich-nanostructured *n*-Cu_2O/AuAg/*p*-Cu_2O Photocathode with Highly Positive Onset Potential for Improved Water Reduction

Yu-Chang Lin,[†] Liang-Ching Hsu,[‡] Chia-Yu Lin,[§] Chao-Lung Chiang,[‡] Che-Min Chou,[‡] Wen-Wei Wu,[†] San-Yuan Chen,*[,†,¶] Yan-Gu Lin*[,‡]

[†]Department of Material Science and Engineering, National Chiao Tung University, Hsinchu 30010, Taiwan

[‡]National Synchrotron Radiation Research Center, Hsinchu 30076, Taiwan

[§]Department of Chemical Engineering, National Cheng Kung University, Tainan 70101, Taiwan

[¶]Frontier Research Center on Fundamental and Applied Sciences of Matters, National Tsing Hua University, Hsinchu 30013, Taiwan

KEYWORDS: solar water splitting; sandwich structure; copper(I) oxide; photocathode; localized surface-plasmon resonance.

Corresponding Author: *E-mail: sanyuanchen@mail.nctu.edu.tw (Prof. San-Yuan Chen); *E-mail: lin.yg@nsrrc.org.tw (Dr. Yan-Gu Lin).

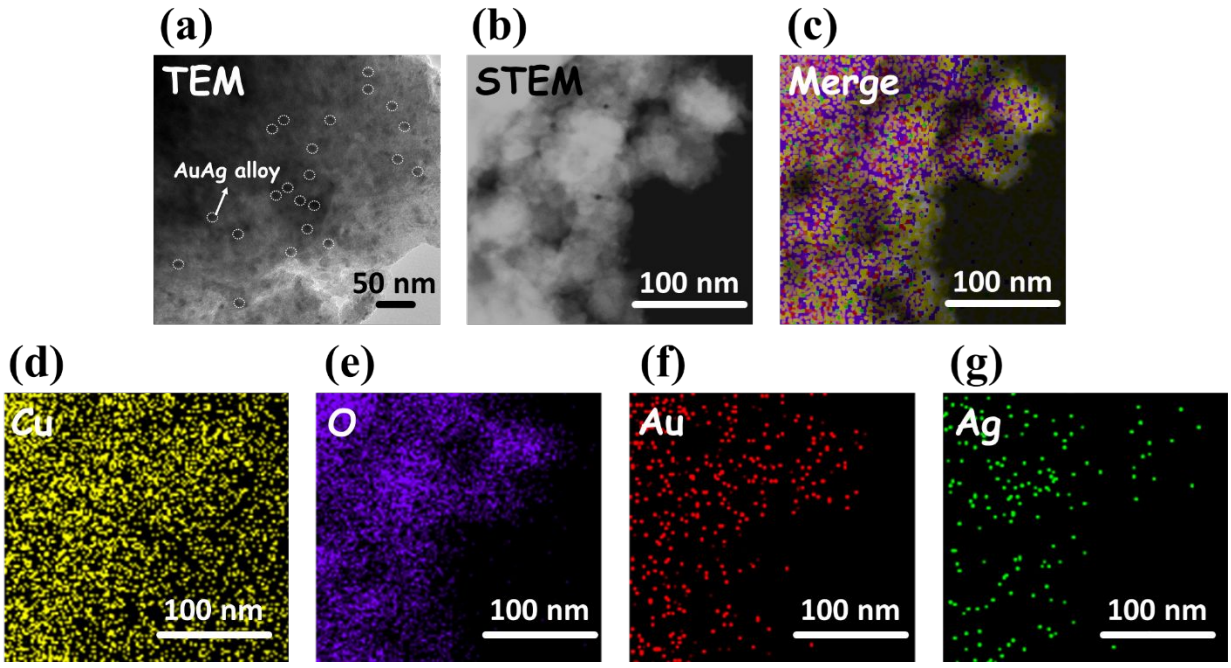

Figure S1. (a) TEM, (b) STEM images of an as-prepared *n*-Cu_2O/AuAg/*p*-Cu_2O with the corresponding element mappings of (c) merge, (d) Cu, (e) O, (f) Au, and (g) Ag.

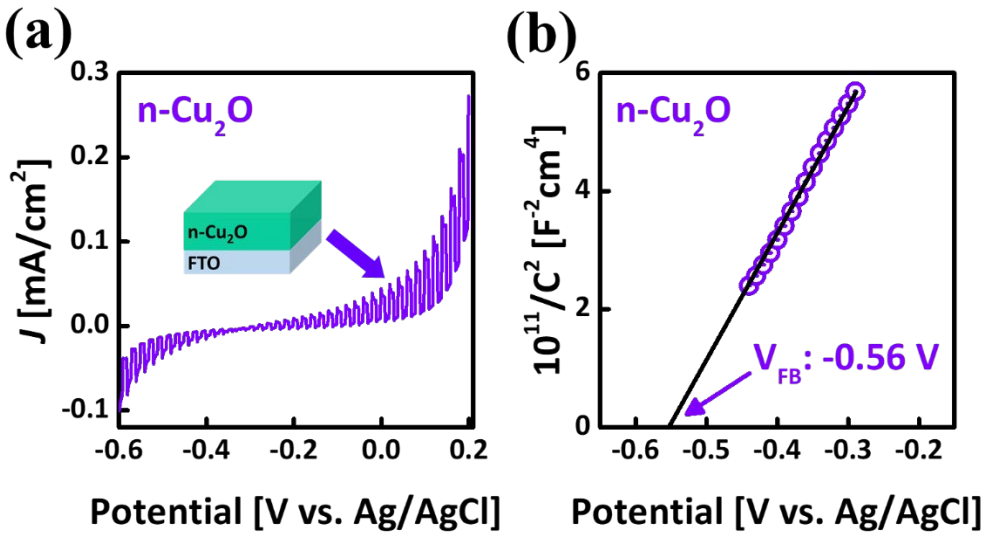

Figure S2. (a) *n*-Cu_2O with LSV measured under chopped light (100 mW cm^{-2}). The arrow shows the position where a transition from anodic photocurrent to cathodic photocurrent is observed. (b) Mott−Schottky plot of n-Cu_2O. A 0.5 M Na_2SO_4 solution was used as the electrolyte for these measurements.

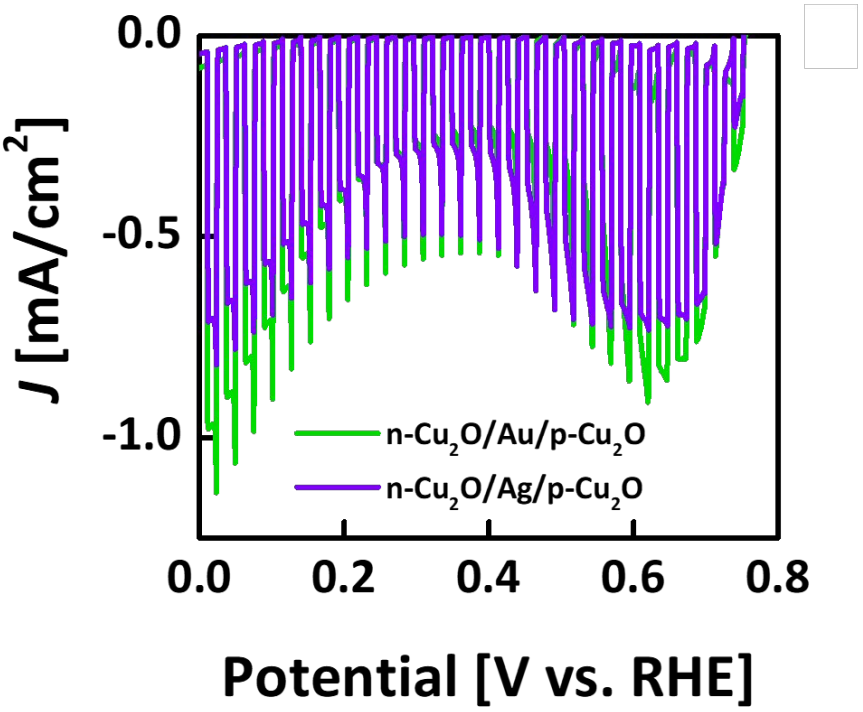

Figure S3. Photocatalytic activities of *p-n* homojunction with Au and Ag plasmonic NPs insertion under chopped AM 1.5 G illumination.

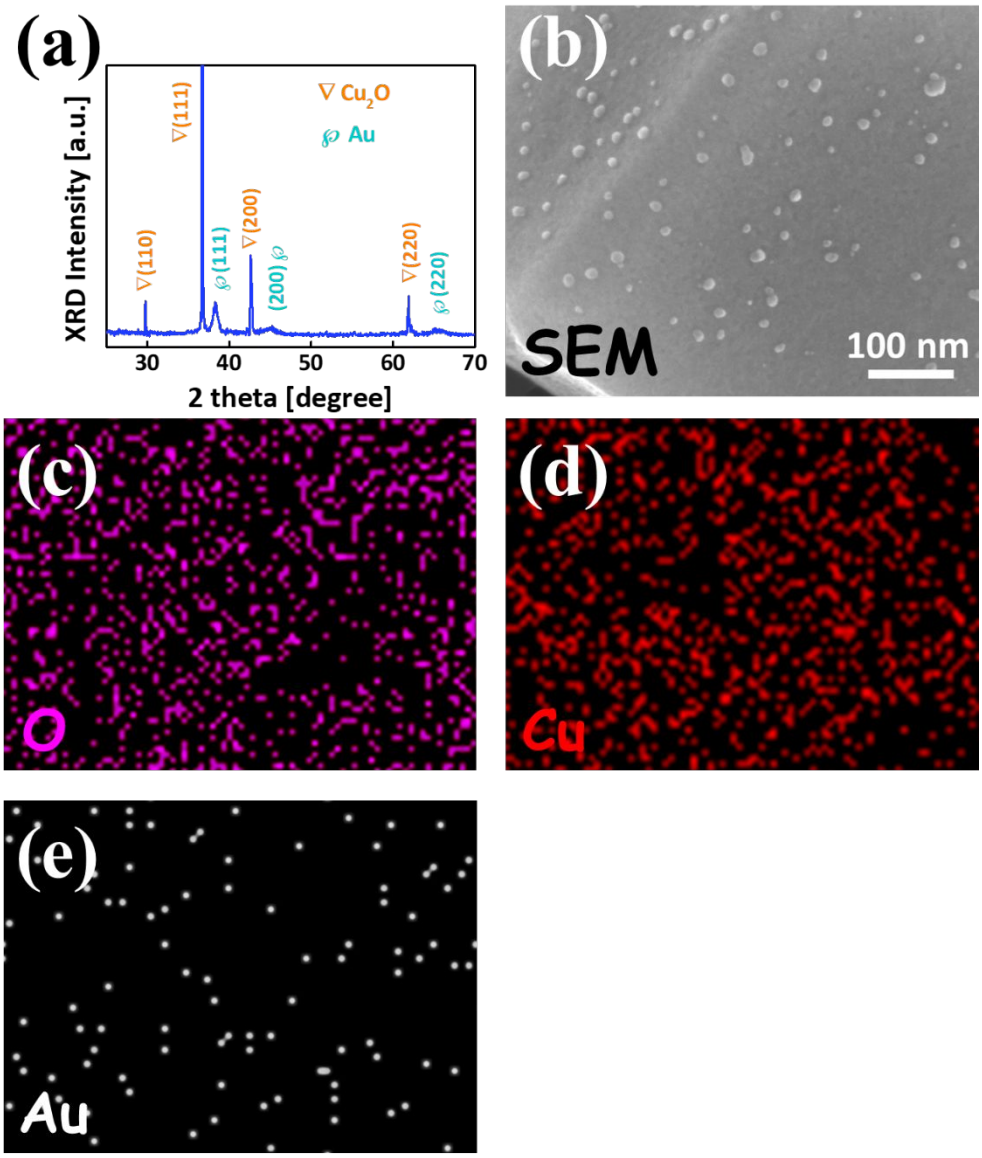

Figure S4. (a) XRD data of *n*-Cu_2O/Au/*p*-Cu_2O photocathode. (b) A SEM image of a top view for Au NPs atop *p*-Cu_2O with the corresponding elemental mapping images of (c) O, (d) Cu, and (e) Au.

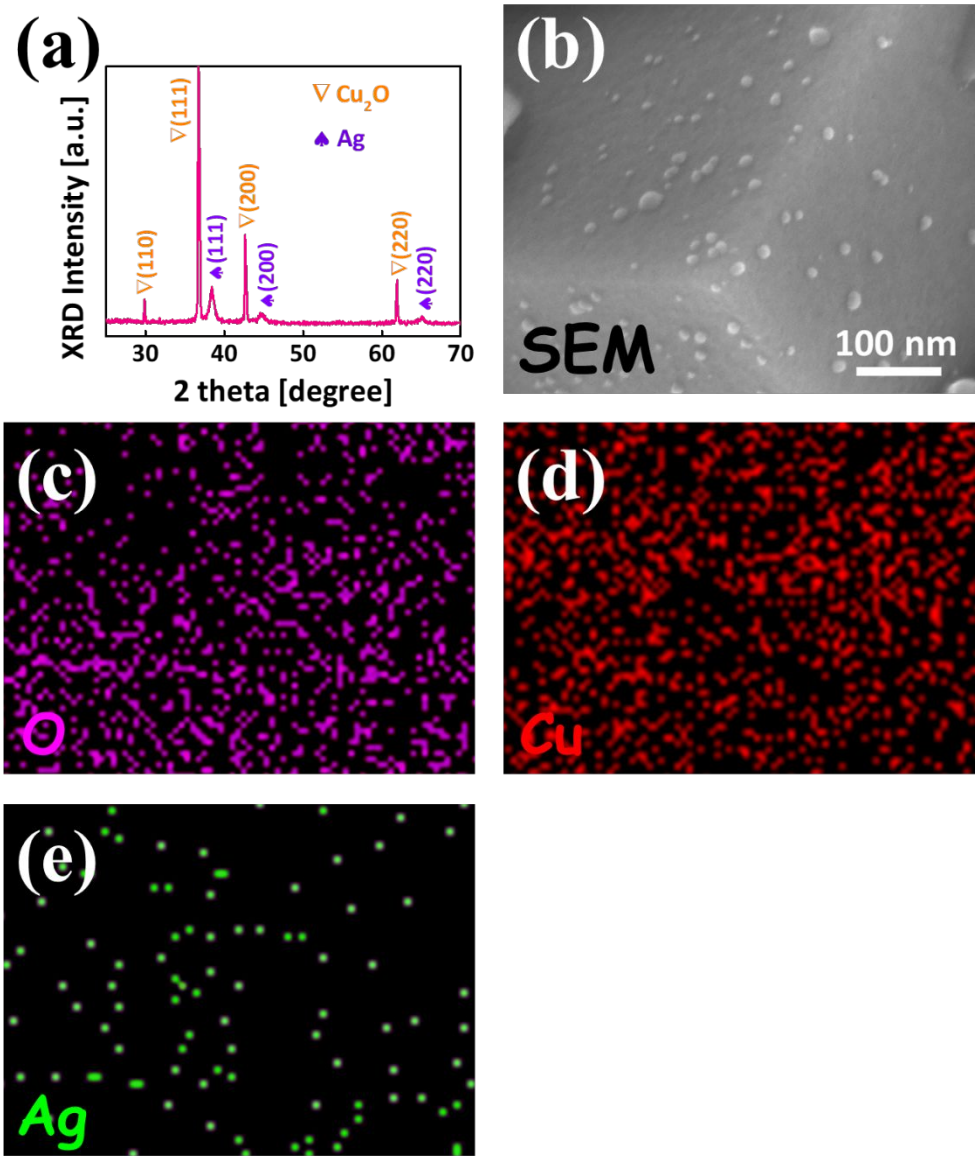

Figure S5. (a) XRD data of *n*-Cu_2O/Ag/*p*-Cu_2O photocathode. (b) A SEM image of a top view for Ag NPs atop *p*-Cu_2O with the corresponding elemental mapping images of (c) O, (d) Cu, and (e) Ag.

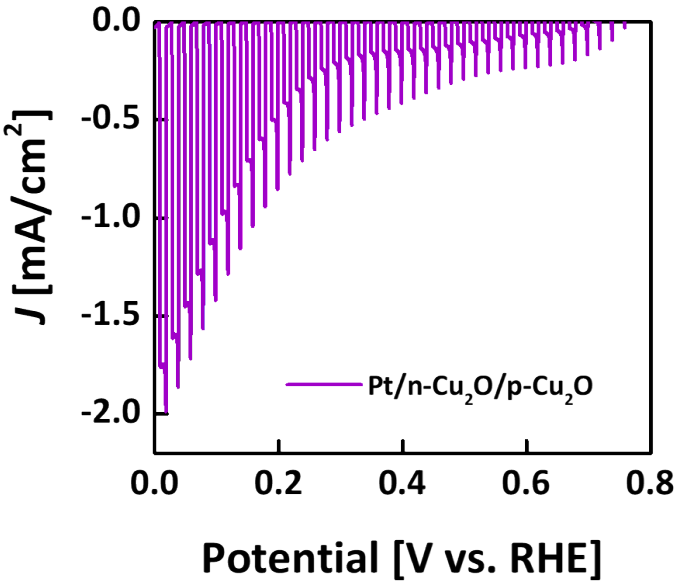

Figure S6. Pt/*n*-Cu_2O/*p*-Cu_2O with LSV measurement under chopped light illumination (100 mW/cm^2). A 0.5 M Na_2SO_4 solution was used as the electrolyte for this measurement.

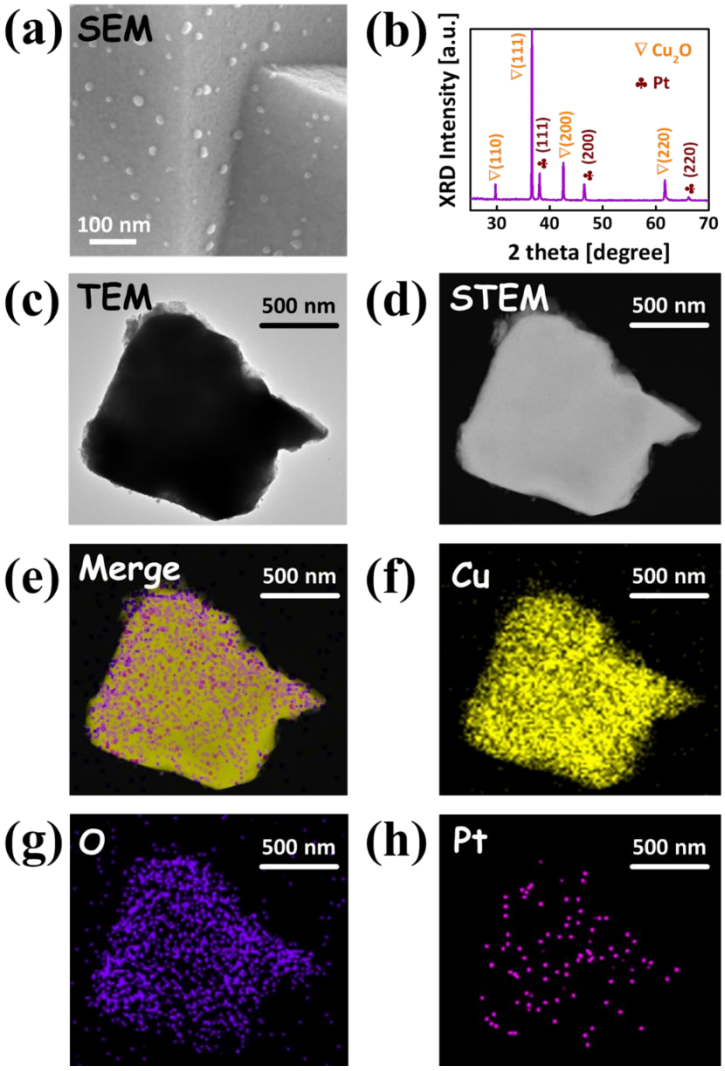

Figure S7. (a) SEM image of Pt NPs deposited dispersedly atop the *n*-Cu_2O/*p*-Cu_2O. (b) XRD patterns of Pt/*n*-Cu_2O/*p*-Cu_2O photocathode. (c) TEM, (d) STEM images of Pt/*n*-Cu_2O/*p*-Cu_2O with the corresponding element mappings of (e) merge, (f) Cu, (g) O, and (h) Pt.

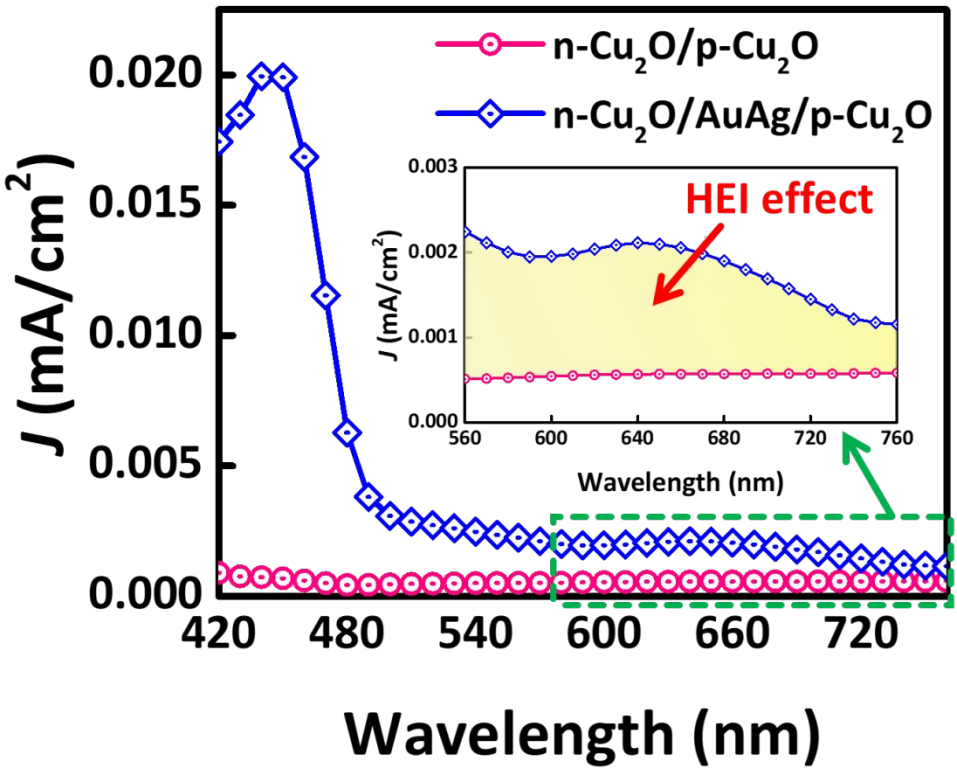

Figure S8. Wavelength-dependent photocatalytic activity of *n*-Cu_2O/AuAg/*p*-Cu_2O and *n*-Cu_2O/*p*-Cu_2O photocathodes measured at applied bias of 0.7 V_{RHE}.

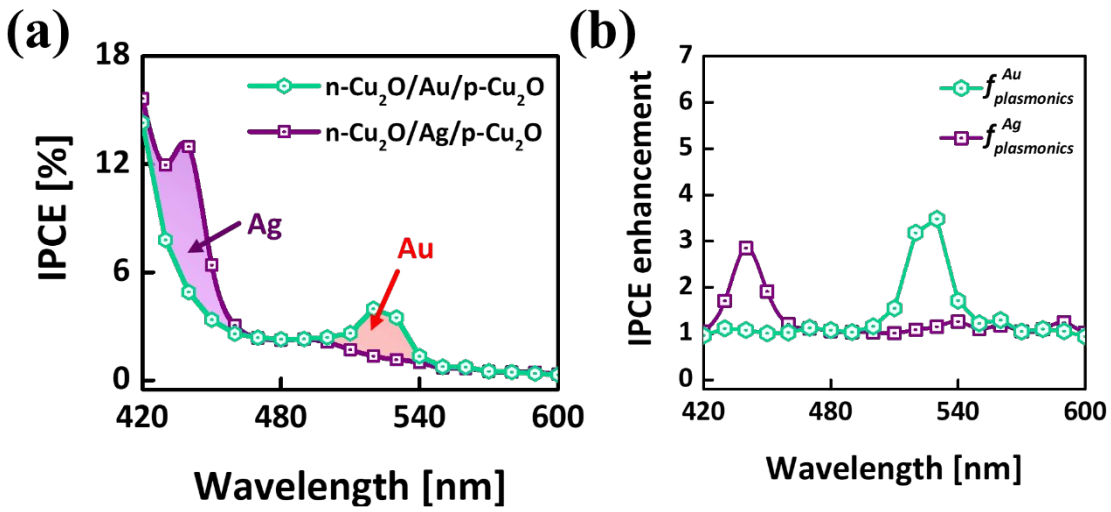

Figure S9. (a) IPCE characteristics and (b) IPCE enhancement spectra of *n*-Cu_2O/Au/*p*-Cu_2O and *n*-Cu_2O/Ag/*p*-Cu_2O photocathodes measured at applied bias of 0.7 V_{RHE}.

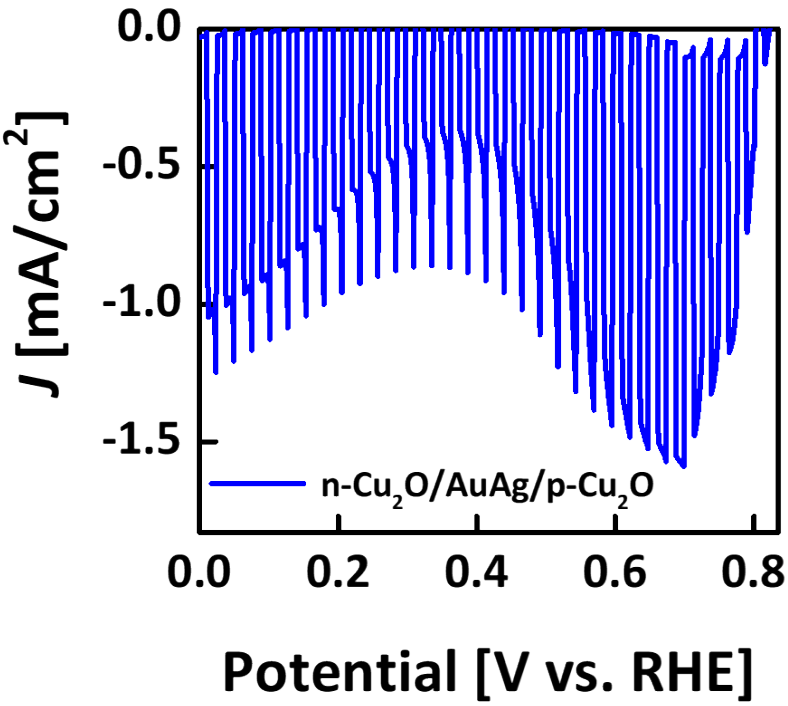

Figure S10. *n*-Cu_2O/AuAg/*p*-Cu_2O with LSV measurement under chopped light illumination (100 mW/cm^2). A 0.5 M Na_2SO_4 solution was used as the electrolyte for this measurement.

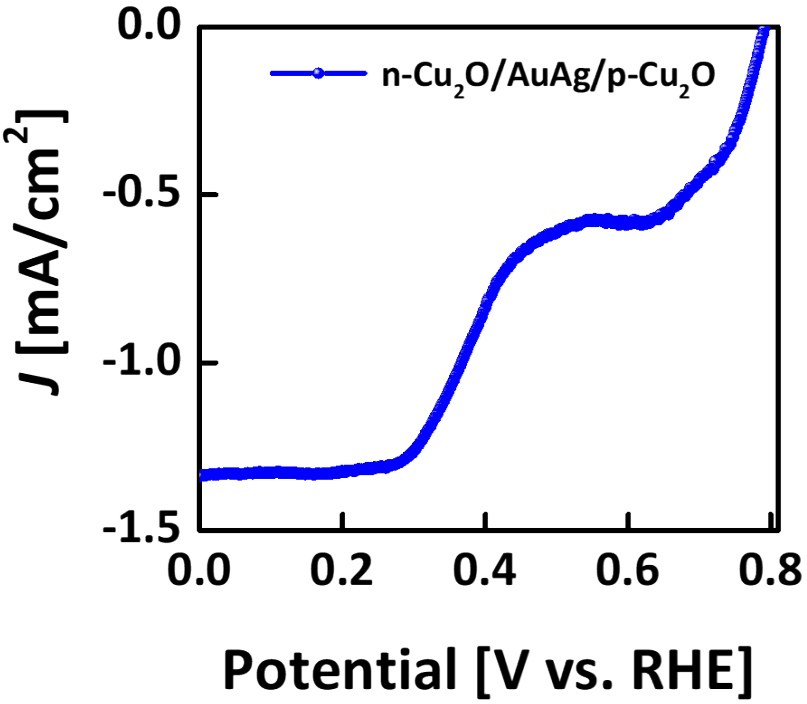

Figure S11. LSV measurement of the *n*-Cu_2O/AuAg/*p*-Cu_2O under consecutive light illumination (100 mW/cm^2). A 0.5 M Na_2SO_4 solution was used as the electrolyte for this measurement.

The amount of hydrogen generation was detected and quantified by headspace gas analysis with Agilent 7890A Series gas chromatography (GC) equipped with a 5 Å molecular sieve column (N_2 carrier gas at a flow rate of approximately 3 mL min^{-1}). The temperature in a GC oven was measured with a thermal conductivity detector that was kept at 40 ℃. The electrochemical cell was purged with 2% CH_4 in N_2 for at least 30 min before PEC experiments; methane is used as an internal standard for H_2 quantification by gas chromatography (GC). A 2.7 mL aliquots of the headspace gas was removed from the air-light electrochemical cell for GC analysis after applying the charge of 0.05 C (at 0.0 V vs. RHE for three-electrode system).[60]

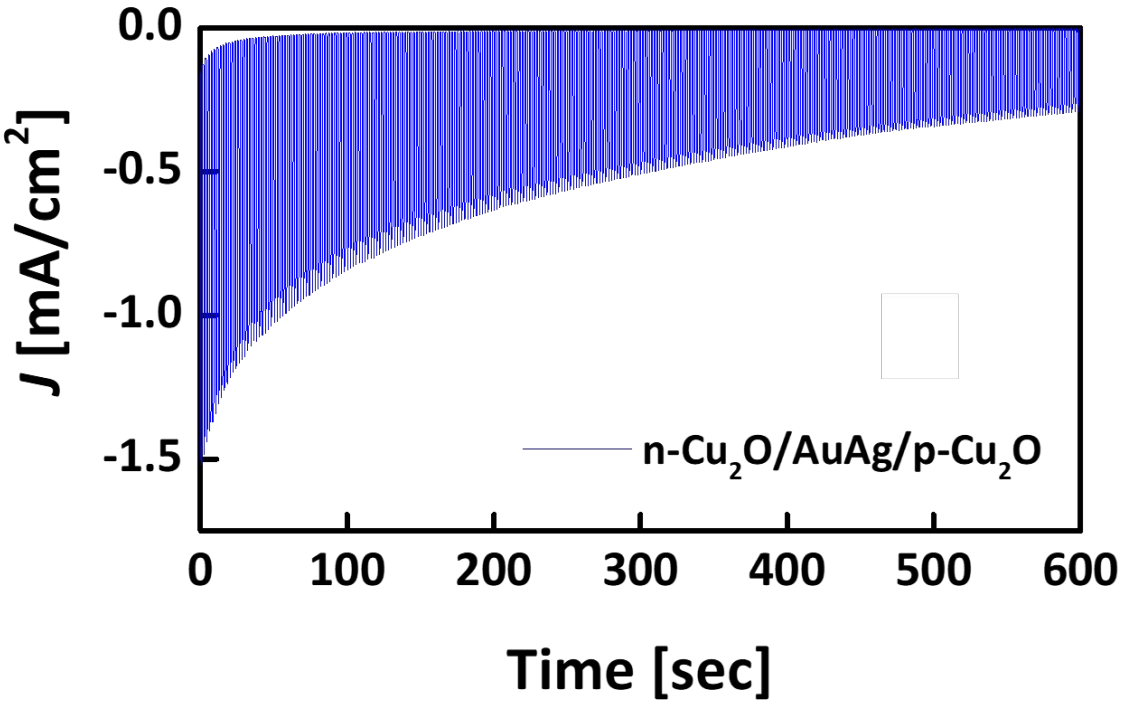

Figure S12. Stability of *n*-Cu_2O/AuAg/*p*-Cu_2O was examined using a chronoamperometry technique at a constant potential (0 V_{RHE}) under chopped light illumination (100 mW/cm^2) in a 0.5 M Na_2SO_4 electrolyte.

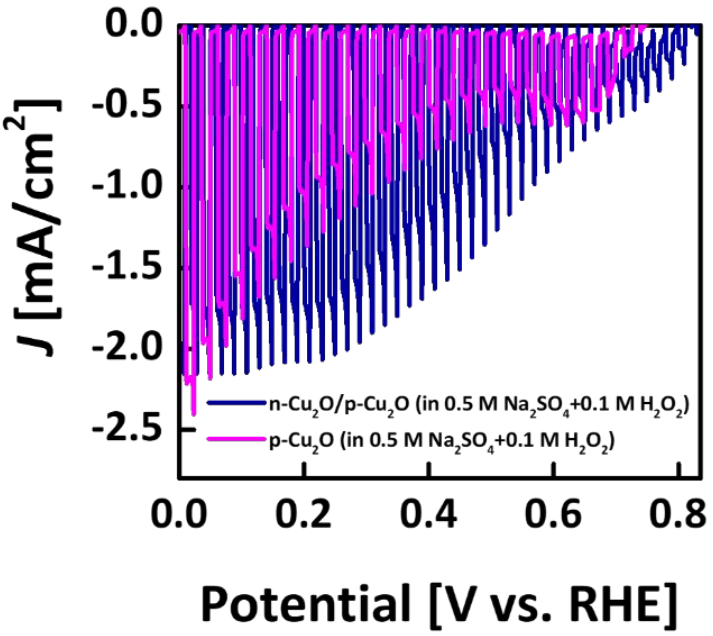

Figure S13. The LSV measurements of *p*-Cu_2O and *n*-Cu_2O/*p*-Cu_2O in the presence of H_2O_2 sacrificial solution under chopped light (100 mW/cm^2).

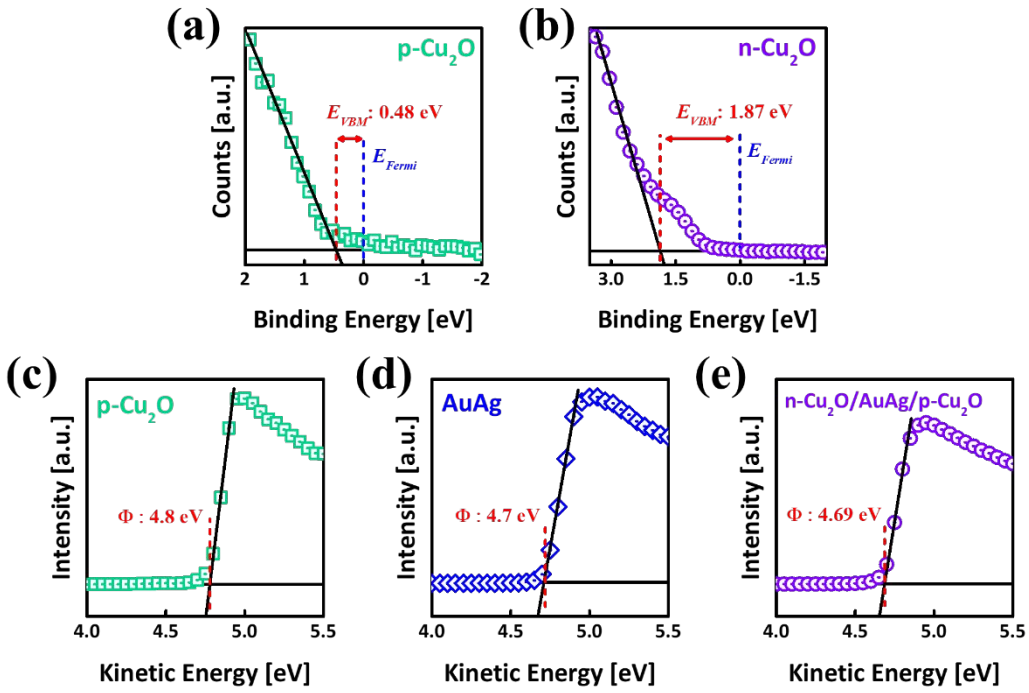

Figure S14. Valence band XPS spectrum of (a) *p*-Cu_2O and (b) *n*-Cu_2O in the region of the valence band maximum. The binding energy scale is with respect to the Fermi level (E_{Fermi}). The valence band maximum occurs at the intersection of a line fit to the linear portion of the leading edge and the extended background line between the valence band maximum and the Fermi level. The work function of (c) *p*-Cu_2O, (d) AuAg, and (e) *n*-Cu_2O/AuAg/*p*-Cu_2O electrodes measured from ultraviolet photoelectron spectrum (UPS).

Table S1. Comparison of the reported photocathodes' onset potential.

Photocathode	Onset Potential	Ref.
n-Cu_2O/AuAg/*p*-Cu_2O	0.8 V_{RHE}	This work
Pt/ZnO/Al_2O_3/TiO_2/Cu_2O/Au	~ 0.5 V_{RHE}	[08]
Pt/TiO_2/ZnS/Cu_2O/Au	0.72 V_{RHE}	[09]
RuO_x/TiO_2/AZO/Cu_2O/Au	0.55 V_{RHE}	[10]
RuO_2/TiO_2/AZO/Cu_2O/Au	0.5 V_{RHE}	[11]
Pt/TiO_2/Ga_2O_3/Cu_2O	1.02 V_{RHE}	[12]
Pt/TiO_2/Ga_2O_3/Cu_2O	1.0 V_{RHE}	[13]
RuO_x/TiO_2/AZO/Cu_2O NWs	0.48 V_{RHE}	[14]
TiO_2/CuO/Cu_2O NWs	~ 0.45 V_{RHE}	[16]
ZnO/Cu_2O/Ag	~ 0.4 V_{RHE}	[37]
$(PEI/NiPOM)_n$/Cu_2O/Au	~ 0.5 V_{RHE}	[45]
RuO_x/TiO_2/Ga_2O_3/Cu_2O NWs	1.0 V_{RHE}	[51]
Graphene/Cu_2O/Cu mesh	~ 0.55 V_{RHE}	[55]
Ni/CuO/Cu_2O	~ 0.55 V_{RHE}	[56]
CuO/Cu_2O bilayered composite	~ 0.8 V_{RHE}	[57]
Pt/Cu_2O/Au	~ 0.6 V_{RHE}	[58]
BFO/Au/Cu_2O	1.01 V_{RHE}	[59]